Non-Newtonian flow of dilute ferrofluids in a uniform magnetic field

Huei Chu Weng,[1] Chieh-Li Chen,[1] and Cha'o-Kuang Chen[2,*]
[1]*Department of Aeronautics and Astronautics, National Cheng Kung University, Tainan 70101, Taiwan, Republic of China*
[2]*Department of Mechanical Engineering, National Cheng Kung University, Tainan 70101, Taiwan, Republic of China*
(Received 20 January 2008; published 14 November 2008)

Nonequilibrium magnetization states predict non-Newtonian ferrofluid properties. It is desirable to understand the corresponding flow fields and characteristics. In this study, we derive a magnetoviscosity expression coming from the effective-field method and describing the shear-thinning non-Newtonian behavior of dilute ferrofluids with finite magnetic anisotropy. A mathematical model is developed of non-Newtonian plane flow with respect to shear and pressure driving mechanisms in the presence of an applied stationary uniform magnetic field oriented in the direction perpendicular to vorticity. The results reveal that the non-Newtonian effect tends to increase the velocity and angular velocity but to reduce the magnetization strength. Moreover, an enhanced flow rate and reduced flow drag may be obtained. The maximum non-Newtonian effect is found at a ratio of the Néel relaxation time to the Brownian relaxation time of the order of 0.1.

DOI: 10.1103/PhysRevE.78.056305 PACS number(s): 47.65.Cb, 47.50.−d, 66.20.Ej, 83.60.Rs

I. INTRODUCTION

Dispersions of nanometric ferrimagnetic or ferromagnetic particles (magnetic nanofluids) exhibit so-called superparamagnetic behavior in the presence of an applied magnetic field [1,2]. In colloids, magnetic nanoparticles are usually covered with a surfactant layer or polymer molecular layer to prevent agglomeration. Neuringer and Rosensweig [3] called these magnetic nanocolloids "ferrofluids," a name that conveys their combination of magnetic response and liquid state. Since the properties and the location of these fluids can easily be influenced by an external magnetic field, they have recently attracted many scientific, industrial, and commercial applications such as magnetofluidic seals, lubricants, density separation, ink jet printers, refrigeration, diagnostics in medicine, clutches, tunable dampers, etc. [4–9]. A fundamental understanding of flow fields and characteristics of ferrofluids, which may deviate from those for nonmagnetic fluids or Newtonian fluids (fluids for which the shear stress is linearly related to the strain rate), is required for the technological demands.

When a magnetic field is applied, magnetic nanoparticles in fluids tend to remain rigidly aligned with the direction of the orienting field. As a result, the viscous dissipation increases. McTague [10] observed that the effective viscosity of ferrofluids in capillary flow is a function of the direction of the applied uniform field. Under the action of a magnetic field applied in the parallel and the perpendicular directions of the flow, his viscosity measurements showed that the viscosity increases with the field in both the configurations and that the increment in the parallel configuration is greater by a factor of 2 than that in the perpendicular configuration. Considering the internal spin of dilute ferrofluids, Shliomis [11] (Sh72) later obtained a set of hydrodynamic equations (the mass and momentum balance equations, the Maxwell equations, and the magnetization equation) and analytically derived a magnetoviscosity expression for plane Couette flow under a uniform magnetic field oriented in the perpendicular direction of vorticity. Furthermore, an anisotropic one was obtained, so as to satisfy McTague's observation. Martsenyuk-Raikher-Shliomis [12] (MRSh) later proposed another magnetization equation derived microscopically from the Fokker-Planck (FP) equation [13,14]. Tsebers [15,16] performed the numerical simulation of magnetic moment dynamics and indicated that the MRSh model using the effective-field (EF) method proposed by Leontovich [17] perfectly describes the magnetization in wide ranges of ξ and $\varpi\tau$, where ξ is the dimensionless magnetic-field strength, ϖ is the fluid vorticity, and τ is the relaxation time. Shliomis *et al.* [18] came to the same conclusion by comparing the results of tangential magnetostress under the EF-method-based MRSh model with those obtained by numerical integration of the FP equation. In this work, they also indicated that non-Newtonian properties can be predicted in nonequilibrium magnetization states with finite values of $\varpi\tau$ and that the Sh72 model is valid only for $\varpi\tau \to 0$ (weakly nonequilibrium states), a case in which Newtonian behavior prevails. Recently, Felderhof [19,20] (Feld), Shliomis [21] (Sh01), Müller and Liu [22] (ML), and Weng and Chen [23] (WC) proposed modifications in the magnetization equation, so as to obtain a more proper form than the Sh72 model or a simpler form than the MRSh model. Comparing with magnetoviscosity measurements of Poiseuille flow of ferrofluids in a stationary cylinder with $\varpi\tau \to 0$ (a low-pressure-gradient pump), Patel *et al.* [24] demonstrated that the Feld model should be avoided. Comparing with transverse magnetization measurements of a ferrofluid in a rotating cylinder with large values of $\varpi\tau$ (high rotational frequencies), Embs *et al.* [25] showed with amplitude correction factors that the Feld and Sh01 models should be avoided and the ML model for the weak-field case with proper coefficient setting [26] should be preferred. On the basis of a more exact insight into the hydrodynamic problem of rotating ferrofluids, Weng and Chen [23] argued for the reduced forms of the magnetization equations shown in their work and concluded that the Feld and ML models should be avoided and that the Sh01 and WC models, which are simpler than the MRSh model, should be preferred.

*ckchen@mail.ncku.edu.tw

Despite a long research history over the past decades, there is no full understanding of the hydrodynamics of non-Newtonian ferrofluids in the presence of an applied uniform magnetic field. Non-Newtonian flow of dilute ferrofluids in wide ranges of ξ and $\varpi\tau$ should be studied extensively. In this paper, we study the planar flow of dilute ferrofluids with finite magnetic anisotropy in a stationary uniform magnetic field oriented in the perpendicular direction of vorticity. The main goal is to obtain a mathematical model and to understand the physical aspects of general viscometric flows. A magnetoviscosity expression describing the non-Newtonian behavior is first derived from the MRSh model by the EF method. The corresponding fully developed field equations with respect to shear and pressure driving mechanisms are further analytically derived. By comparing with available Newtonian-fluid models, the applicability of the EF magnetoviscosity for small and moderate values of ξ is discussed. According to the stress-strain relation, the fluid regime is determined. The non-Newtonian effect on the flow fields and characteristics, including the velocity, angular velocity, cross-flow magnetization, streamwise magnetization, flow rate, and flow drag, is studied.

II. PROBLEM FORMULATIONS

A. Field equations

The set of hydrodynamic equations for incompressible dilute ferrofluids under the effective-field method [17] consists of the mass balance equation

$$\nabla \cdot \mathbf{v} = 0, \tag{1}$$

the linear momentum balance equation

$$\rho\frac{d\mathbf{v}}{dt} = -\nabla p + (\mu+\kappa)\nabla^2\mathbf{v} + 2\kappa(\nabla\times\boldsymbol{\omega}) + \frac{1}{2}(\nabla\mathbf{h}_0)\cdot\mathbf{m} - \frac{1}{2}(\nabla\mathbf{m})\cdot\mathbf{h}_0, \tag{2}$$

the angular momentum balance equation

$$\rho j\frac{d\boldsymbol{\omega}}{dt} = -4\kappa(\boldsymbol{\omega}-\hat{\boldsymbol{\omega}}) + \mathbf{m}\times\mathbf{h}_0, \tag{3}$$

the Maxwell equations

$$\nabla\cdot\mathbf{b} = 0, \quad \nabla\times\mathbf{h}_0 = \mathbf{0}, \tag{4}$$

and the magnetization equation (MRSh model) [12]

$$\frac{d\mathbf{m}}{dt} + \mathbf{m}\times\boldsymbol{\omega} = \frac{\mathbf{m}[\mathbf{h}_e\cdot(\mathbf{h}_0-\mathbf{h}_e)]}{\tau|\mathbf{h}_e|^2} - \frac{\mathbf{h}_e\times(\mathbf{m}\times\mathbf{h}_0)}{A(\zeta)\tau|\mathbf{h}_e|^2}, \tag{5}$$

where

$$A(\zeta) = \frac{2L(\zeta)}{\zeta - L(\zeta) - \zeta L^2(\zeta)}. \tag{6}$$

The companion constitutive relation is

$$t_{ij} = \mathbf{T} = -\left(p + \frac{1}{2}(\mathbf{h}_0\cdot\mathbf{m})\right)\mathbf{I} + \mu[(\nabla\mathbf{v})^T + \nabla\mathbf{v}] + [\mathbf{b}\mathbf{h}_0 + \mathbf{h}_0\mathbf{b} - (\mathbf{h}_0\cdot\mathbf{h}_0)\mathbf{I}]/8\pi + \mathbf{e}\cdot\left(2\boldsymbol{\kappa}(\hat{\boldsymbol{\omega}}-\boldsymbol{\omega}) + \frac{1}{2}(\mathbf{m}\times\mathbf{h}_0)\right). \tag{7}$$

Here, d/dt is the material derivative, $\mathbf{T}$ is the stress tensor, $\mathbf{I}$ is the Kronecker δ, $\mathbf{e}$ is the third-order alternating pseudotensor, $\mathbf{v}$ is the velocity vector, $\boldsymbol{\omega}$ is the angular velocity vector, p is the pressure, ρ is the density, μ is the shear viscosity, κ is the vortex viscosity, related to μ by $\kappa = 3\mu\varphi/2$, j is the moment of inertia per unit mass, τ is the effective relaxation time, $\mathbf{m}$ is the magnetization vector under the applied external magnetic field vector $\mathbf{h}_0$ and the flow vorticity vector $\hat{\boldsymbol{\omega}}=\nabla\times\mathbf{v}/2$, $\mathbf{b}$ is the induction field vector, related to $\mathbf{h}_0$ and $\mathbf{m}$ by $\mathbf{b}=\mathbf{h}_0+4\pi\mathbf{m}$, and $\mathbf{h}_e$ is the effective field vector, related to $\mathbf{m}$ by

$$\mathbf{m} = m_s L(\zeta)\frac{\boldsymbol{\zeta}}{\zeta} = N\bar{\eta}_m L(\zeta)\frac{\boldsymbol{\zeta}}{\zeta}, \quad N = \varphi/\bar{V}, \quad \boldsymbol{\zeta} = \bar{\eta}_m\mathbf{h}_e/k_B T, \tag{8}$$

where m_s is the saturation magnetization, L is the Langevin function, $\boldsymbol{\zeta}$ ($|\boldsymbol{\zeta}|=\zeta$) is the Langevin argument of the effective field vector (dimensionless effective field vector), N is the particle number per unit volume, φ is the particle volume fraction, $\bar{V}$ is the mean volume per particle, $\bar{\boldsymbol{\eta}}_m$ ($|\bar{\boldsymbol{\eta}}_m|=\bar{\eta}_m$) is the mean magnetic moment vector per particle, k_B is the Boltzmann constant, and T is the absolute temperature. The momentum balance equations (2) and (3) can be found in Hubbard and Stiles [27], and the magnetization equation (5) can be obtained from Shliomis *et al.* [18].

The dynamics of magnetization is linked with two thermal fluctuation mechanisms. The first is the Brownian mechanism. In this mechanism, the relaxation occurs by particle rotation [28] with the characteristic time [29]:

$$\tau_B = \frac{3\bar{V}\mu}{k_B T}. \tag{9}$$

The second is the Néel mechanism. In this mechanism, the relaxation is due to rotation of the magnetic moment within the particle [30]. According to Brown [31], the characteristic time has the form

$$\tau_N = \frac{\sqrt{\pi}}{2}\tau_D\sigma^{-3/2}e^{\sigma}, \quad \tau_D = \sigma\tau_0 = \frac{3\bar{V}_m\mu_m}{k_B T}. \tag{10}$$

This expression is the asymptote for $\sigma \gg 1$. Using a combination of a variational principle and a curve fitting, Cregg *et al.* and Coffey *et al.* [32,33] suggested a formula for the full range of σ:

$$\tau_N = \tau_D\frac{e^{\sigma}-1}{2\sigma}\left(\frac{\sigma\sqrt{\sigma/\pi}}{1+\sigma} + 2^{-\sigma-1}\right)^{-1}. \tag{11}$$

Here, τ_0 is the extinction time of the Larmor precession, $\bar{V}_m$ is the mean volume of the magnetic phase per particle, $\mu_m = m_l/6\alpha\gamma$ is the magnetic viscosity (m_l is the saturation magnetization of the ferromagnet, α is a dimensionless attenua-

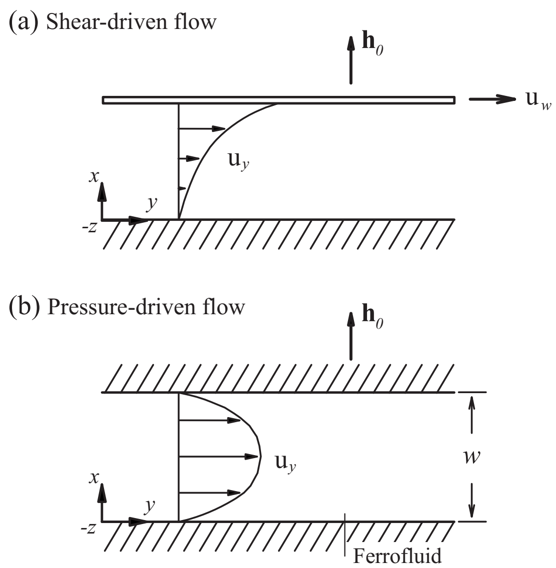

FIG. 1. Two fundamental mechanisms of ferrohydrodynamic driving in the presence of an applied uniform magnetic field.

tion constant of the precession of the magnetic moment in the effective field, and γ is the gyromagnetic ratio), and $\sigma = K\bar{V}_m/k_BT$ is the height of the potential barrier of magnetic anisotropy (K is the energy density of the effective magnetic anisotropy). The magnetic moment of a particle is coupled with the particle body due to the energy of magnetic anisotropy $K\bar{V}_m$. In the case where $K\bar{V}_m$ is much greater than the thermal energy k_BT ($\tau_N/\tau_B \to \infty$), the magnetic moment vector is aligned strictly along the axis of easy magnetization. The particle represents a hard magnetic dipole. Any change of particle orientation is possible only by Brownian rotation of the particle. For the case of $K\bar{V}_m \sim k_BT$ ($\tau_N/\tau_B \sim 1$), this means that, for a finite value of magnetic anisotropy, the magnetic moment vector is only partly frozen. Thus, it can turn within the particle body. The Néel mechanism may then play an important role in magnetization relaxation. The two relaxation mechanisms described above occur in parallel and therefore the effective relaxation time takes the form [25,34,35]

$$\tau = \frac{1}{1/\tau_B + 1/\tau_N} = \frac{\Gamma}{\Gamma + 1}\tau_B, \tag{12}$$

where Γ is the magnetic-anisotropy parameter, defined as the ratio of the Néel relaxation time to the Brownian relaxation time.

B. Magnetoviscosity

Below, we propose a magnetoviscosity model which could be applicable to dilute ferrofluids with finite magnetic anisotropy in nonequilibrium magnetization states. Let x, y, and z denote the usual rectangular coordinates. Consider a steady flow through a parallel-plate channel of width w in the presence of an applied stationary uniform magnetic field $\mathbf{h}_0 = (h_0, 0, 0)$, as shown in Fig. 1. For a sufficiently long channel, we assume that the fully developed condition can be achieved in the form

$$\mathbf{v} = (0, u_y(x), 0), \quad p = p(x,y),$$

$$\boldsymbol{\omega} = (0, 0, \omega_z(x)),$$

$$\mathbf{m} = (m_x(x), m_y(x), 0). \tag{13}$$

The constitutive equation described by Eq. (7) then reduces to

$$t_{ij} = \mathbf{T} = -\left(p + \frac{\mathbf{h}_0 \cdot \mathbf{m}}{2} + \frac{\mathbf{h}_0 \cdot \mathbf{h}_0}{8\pi}\right)\mathbf{I} + \mu[(\nabla\mathbf{v})^T + \nabla\mathbf{v}] + \frac{\mathbf{h}_0\mathbf{h}_0}{4\pi} + \frac{\mathbf{m}\mathbf{h}_0 + \mathbf{h}_0\mathbf{m}}{2}. \tag{14}$$

Thus, the shear stress is

$$t_{xy} = 2(\mu + \mu_{\text{mv}})\hat{\omega}, \tag{15}$$

where $2\varpi = \partial u_y/\partial x$ is the strain rate, and the additional viscosity induced by the magnetic field, the so-called magnetoviscosity, is

$$\mu_{\text{mv}} = \frac{m_y h_0}{4\hat{\omega}}. \tag{16}$$

For extremely small values of $\varpi\tau$, the off-axis component of magnetization, m_y, is a nearly linear function of ϖ [21]. So the shear stress t_{xy} is linearly related to ϖ. As a result, dilute ferrofluids in the limit $\varpi\tau \to 0$ are Newtonian. However, for finite values of $\varpi\tau$, the viscosity $\mu + \mu_{\text{mv}}$ does depend on ϖ. The function $t_{xy}(\varpi)$ deviates from the linear one, i.e., fluids acquire non-Newtonian properties.

Equation (5) admits a steady solution in which the effective field $\mathbf{h}_e$ (with the corresponding Langevin argument $\boldsymbol{\zeta}$, $|\boldsymbol{\zeta}| = \zeta$) tracks the magnetic field $\mathbf{h}_0$ (with the corresponding Langevin argument $\boldsymbol{\xi}$, $|\boldsymbol{\xi}| = \xi$) with lag angle θ, i.e., $\boldsymbol{\zeta} = (\zeta\cos\theta, \zeta\sin\theta, 0)$. The dependence of ζ and θ upon ξ and the $\varpi\tau$ is given by

$$\sqrt{\xi^2 - \zeta^2} = \frac{2(\Gamma + 1)\zeta L(\zeta)}{(\Gamma + 1)\zeta - (\Gamma + 1)L(\zeta) - \zeta L^2(\zeta)}\hat{\omega}\tau, \quad \cos\theta = \zeta/\xi. \tag{17}$$

Substituting $m_y = N\bar{\eta}_m L(\zeta)\sin\theta$ in (16) and using (17), we obtain

$$\mu_{\text{mv}} = \frac{3}{2}\mu\varphi\frac{\Gamma\zeta L^2(\zeta)}{(\Gamma + 1)\zeta - (\Gamma + 1)L(\zeta) - \zeta L^2(\zeta)}. \tag{18}$$

For a magnetic field with arbitrary orientation, the right-hand side of the magnetoviscosity expression should be multiplied by $\sin^2\phi$, where ϕ is the angle between $\mathbf{h}_0$ and $\boldsymbol{\varpi}$.

In Figs. 2–4, we check the results with those for the hard-dipole case $\Gamma \to \infty$ and with those for the Newtonian-fluid (weakly nonequilibrium) case $\varpi\tau \to 0$. Note that Eq. (18) can be reduced to

$$\mu_{\text{mv}} = \frac{3}{2}\mu\varphi\frac{\zeta L^2(\zeta)}{\zeta - L(\zeta)} \quad \text{for } \Gamma \to \infty \tag{19}$$

and

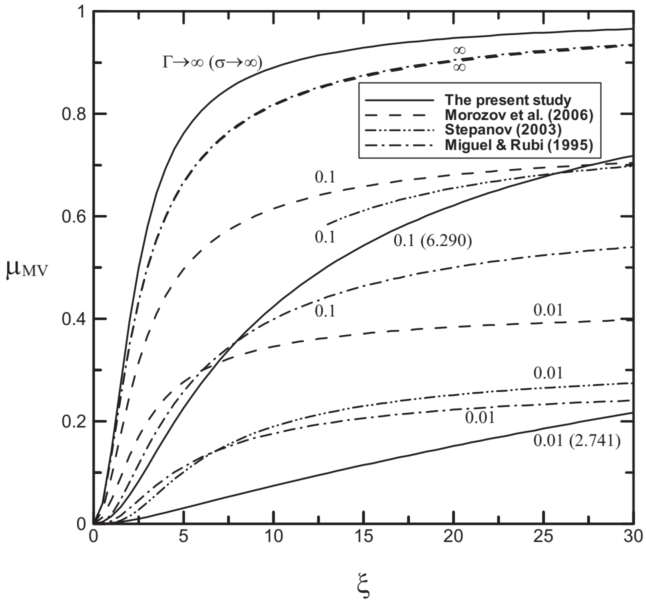

FIG. 2. Variation of the reduced magnetoviscosity μ_{MV} with the dimensionless magnetic field strength ξ for different Newtonian-fluid (weakly nonequilibrium) models with different values of the magnetic-anisotropy parameter σ. The limit of Stepanov's model is $\sigma < \xi/2$.

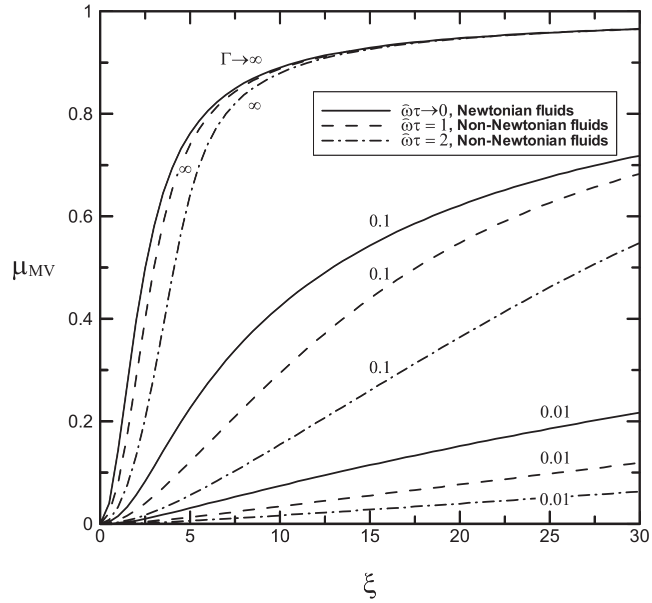

FIG. 3. Variation of the reduced magnetoviscosity μ_{MV} with the dimensionless magnetic-field strength ξ for different values of the shear deformation $\varpi\tau$ with three assigned values of the magnetic-anisotropy parameter Γ.

$$\mu_{\mathrm{mv}} = \frac{3}{2}\mu\varphi \frac{\Gamma \xi L^2(\xi)}{(\Gamma+1)\xi - (\Gamma+1)L(\xi) - \xi L^2(\xi)} \quad \text{for } \hat{\omega}\tau \to 0. \tag{20}$$

Equation (19) is identical to the expression obtained by Shliomis [21]. Equation (20) is later compared with available Newtonian-fluid models.

C. Viscometric flow

A fundamental understanding of viscometric flow fields and characteristics in ferrohydrodynamic systems is necessary. In this section, we obtain the mathematical model first for the shear-driven plane flow and then for the pressure-driven plane flow. By using the form shown in Eq. (13), the governing equations (1)–(5) can be reduced to

$$\left(\mu + \frac{3}{2}\mu\varphi\mu_{\mathrm{MV}}\right)\frac{d^2 u_y}{dx^2} - \frac{\partial p}{\partial y} = 0, \quad \frac{\partial p}{\partial x} = 0,$$

$$\omega_z = \frac{1}{2}(1-\mu_{\mathrm{MV}})\frac{du_y}{dx},$$

$$m_x = \frac{\zeta}{\xi}L(\zeta)N\bar{\eta}_m,$$

$$m_y = \frac{\mu_{\mathrm{MV}}}{\xi}N\bar{\eta}_m\tau_B\frac{du_y}{dx}, \tag{21}$$

where the dimensionless magnetoviscosity $\mu_{\mathrm{MV}} = \mu_{\mathrm{mv}}/(3\mu\varphi/2)$. The general solutions of these equations are

$$u_y = \frac{1}{2\mu}\left(\frac{1}{1+\frac{3}{2}\varphi\mu_{\mathrm{MV}}}\frac{dp}{dy}x^2 + 2A_1 x\right) + A_0, \tag{22}$$

$$\omega_z = \frac{1}{2\mu}(1-\mu_{\mathrm{MV}})\left(\frac{1}{1+\frac{3}{2}\varphi\mu_{\mathrm{MV}}}\frac{dp}{dy}x + A_1\right), \tag{23}$$

$$m_x = \frac{\zeta}{\xi}L(\zeta)N\bar{\eta}_m, \tag{24}$$

$$m_y = \frac{1}{\mu}\frac{\mu_{\mathrm{MV}}}{\xi}N\bar{\eta}_m\tau_B\left(\frac{1}{1+\frac{3}{2}\varphi\mu_{\mathrm{MV}}}\frac{dp}{dy}x + A_1\right), \tag{25}$$

where A_1 and A_2 are arbitrary constants. An important parameter for flow characteristics is the flow rate, given by

$$\dot{q} = \int_0^w u_y dx = \frac{1}{6\mu}\left(\frac{1}{1+\frac{3}{2}\varphi\mu_{\mathrm{MV}}}\frac{dp}{dy}w^3 + 3A_1 w^2\right) + A_0 w. \tag{26}$$

Another important parameter for flow characteristics is the friction force exerted on the wall (flow drag), defined as

$$\hat{t} = \frac{|t_{xy}(0)| + |t_{xy}(w)|}{2} = \frac{1}{2}\left(1 + \frac{3}{2}\varphi\mu_{\mathrm{MV}}\right)\left(|A_1| + \left|\frac{1}{1+\frac{3}{2}\varphi\mu_{\mathrm{MV}}}\frac{dp}{dy}w + A_1\right|\right). \tag{27}$$

Consider the flow with $dp/dy = 0$ between a stationary plate and a moving plate at a constant velocity u_w, as shown in Fig. 1(a). The dimensionless general solutions with no-slip velocity boundary conditions are

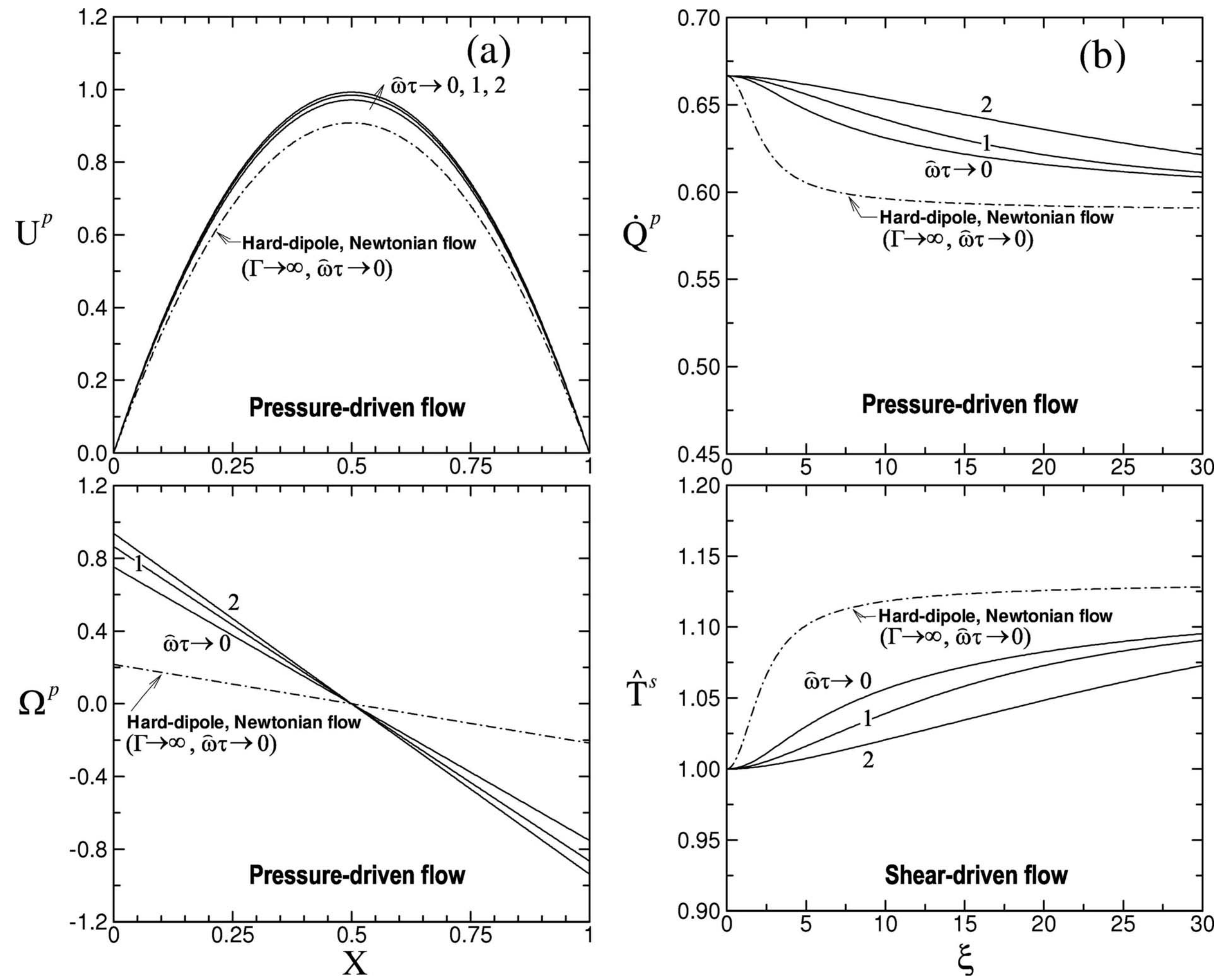

FIG. 4. (a), (b) Velocity and angular velocity U^p, Ω^p versus the position X and flow rate and flow drag $\dot{Q}^p, \hat{T}^s$ versus the magnetic field strength ξ for different values of the shear deformation $\varpi\tau$. The reference values of ξ and Γ used are 5 and 0.1, respectively.

$$U^s = \frac{u_y}{u_w} = X, \tag{28}$$

$$\Omega^s = \frac{\omega_z}{u_w/2w} = 1 - \mu_{\mathrm{MV}}, \tag{29}$$

$$M_x^s = \frac{m_x}{N\bar{\eta}_m} = \frac{\zeta}{\xi}L(\zeta), \tag{30}$$

$$M_y^s = \frac{m_y}{N\bar{\eta}_m\tau_B u_w/w} = \frac{\mu_{\mathrm{MV}}}{\xi}, \tag{31}$$

where

$$X = \frac{x}{w}. \tag{32}$$

The corresponding flow rate and flow drag are, respectively,

$$\dot{Q}^s = \frac{\dot{q}}{u_w w} = \frac{1}{2}, \tag{33}$$

$$\hat{T}^s = \frac{\hat{t}}{\mu u_w/w} = 1 + \frac{3}{2}\varphi\mu_{\mathrm{MV}}. \tag{34}$$

Consider the flow driven by a pressure gradient $-dp/dy$ between two stationary parallel plates, as shown in Fig. 1(b). The dimensionless general solutions with no-slip velocity boundary conditions are

$$U^p = \frac{u_y}{-(w^2/8\mu)dp/dy} = \frac{4}{1+\frac{3}{2}\varphi\mu_{\mathrm{MV}}}(X - X^2), \tag{35}$$

$$\Omega^p = \frac{\omega_z}{-(w/4\mu)dp/dy} = (1-\mu_{\mathrm{MV}})\frac{2}{1+\frac{3}{2}\varphi\mu_{\mathrm{MV}}}\left(\frac{1}{2} - X\right), \tag{36}$$

$$M_x^p = \frac{m_x}{N\bar{\eta}_m} = \frac{\zeta}{\xi}L(\zeta), \tag{37}$$

$$M_y^p = \frac{m_y}{-(N\bar{\eta}_m \tau_B w/8\mu)dp/dy} = \frac{\mu_{MV}}{\xi}\frac{8}{1+\frac{3}{2}\varphi\mu_{MV}}\left(\frac{1}{2} - X\right). \quad (38)$$

The corresponding flow rate and flow drag are, respectively,

$$\dot{Q}^p = \frac{\dot{q}}{-(w^3/8\mu)dp/dy} = \frac{2/3}{1+\frac{3}{2}\varphi\mu_{MV}}, \quad (39)$$

$$\hat{T}^p = \frac{\hat{t}}{-(w/8)dp/dy} = 4. \quad (40)$$

III. RESULTS AND DISCUSSION

We pay attention to the non-Newtonian influence of magnetoviscosity on plane flow for a kerosene-based ferrofluid with magnetite particles (Fe_3O_4) stabilized by a chemisorbed monomolecular layer of pure oleic acid at room temperature (T=298.15 K). The ferrofluid possesses the following properties: shear viscosity $\mu=1.69\times10^{-3}$ kg/m s, the dimensionless attenuation constant $\alpha=4.00\times10^{-2}$, the gyromagnetic ratio $\gamma=2.00\times10^{11}$ 1/T s, the particle volume fraction $\varphi=8.85\times10^{-2}$, the mean magnetic moment strength per particle $\bar{\eta}_m=4.12\times10^{-19}$ A m^2, and the mean volume per particle $\bar{V}=1.77\times10^{-24}$ m^3. Calculations yield $\tau_B=2.18\times10^{-6}$ s and $\tau_D=6.26\times10^{-9}$ s. The parametric study has been performed over the ranges $0\leqslant\xi\leqslant30$, $0<\hat{\omega}\tau\leqslant2$, and $0.01\leqslant\Gamma<\infty$ $(2.741\leqslant\sigma<\infty)$. Note that $\hat{\omega}\tau\to0$ means that the value of $\hat{\omega}\tau$ is much smaller than 0.01 and represents the Newtonian flow and that $\Gamma\to\infty$ means that the value of Γ is much greater than 100 and represents the hard-dipole flow.

First, we compare the calculated results of our magnetoviscosity expression with those of available expressions. Two well-known expressions, obtained phenomenologically by Shliomis [11] and microscopically from the Fokker-Planck equation by Martsenyuk *et al.* [12], are limited to the case of hard dipoles. A number of microscopic expressions based on the FP equation were further developed for the case of particles with finite magnetic anisotropy. Raikher and Shliomis [36] proposed the FP equation for the limit $\sigma\ll\xi$, in which the dipoles are rapidly oriented toward the field direction, and gave calculations of the magnetoviscosity for strong magnetic fields. Shliomis and Stepanov [37] deduced the general FP equation for the case of arbitrary values of σ and obtained the expressions for the weak and strong magnetic fields ($\xi\ll1$ and $\xi\to\infty$):

$$\mu_{mv} = \begin{cases} \frac{1}{4}\mu\varphi\left(\frac{1}{3}[1+2F_2(\sigma)]\frac{\Gamma}{\Gamma+1} + \frac{2}{3}[1-F_2(\sigma)]\frac{\Gamma}{\Gamma+G(\sigma)}\right)\xi^2 & \text{for } \xi\ll1, \\ \frac{3}{2}\mu\varphi\dfrac{\frac{\Gamma\sigma}{G(\sigma)}[14+5F_2(\sigma)+16F_4(\sigma)] + 35\left(1-\frac{\Gamma\sigma}{G(\sigma)}\right)F_2^2(\sigma)}{\left(1+\frac{\Gamma\sigma}{G(\sigma)}\right)[14+5F_2(\sigma)+16F_4(\sigma)] - 35\frac{\Gamma\sigma}{G(\sigma)}F_2^2(\sigma)} & \text{for } \xi\to\infty, \end{cases} \quad (41)$$

where

$$G(\sigma) = \frac{\sqrt{\pi}}{4}\frac{2+F_2(\sigma)}{1-F_2(\sigma)}\sigma^{-3/2}e^{\sigma}, \quad R = \int_0^1 \exp(\sigma x^2)dx, \quad F_2(\sigma) = \frac{3}{2}\left(\frac{dR/d\sigma}{R} - \frac{1}{3}\right), \quad F_4(\sigma) = \frac{1}{8}\left(3 - 30\frac{dR/d\sigma}{R} + 35\frac{d^2R/d^2\sigma}{R}\right). \quad (42)$$

The limits $\xi\ll1$ and $\xi\to\infty$ greatly reduce the applicability of Eq. (41) in the most interesting and widely used region $\xi<10$. Miguel and Rubí [38] used a Green-Kubo equation proposed from linear response theory to obtain the general expression

$$\mu_{mv} = \frac{3}{2}\mu\varphi\xi^2 \lim_{s\to0}\frac{(A_{22}A_{33}-A_{23}A_{32})R_1^0(\xi) - A_{12}A_{33}R_2^0(\xi) + A_{12}A_{23}R_3^0(\xi)}{|(A_{ij})|}, \quad (43)$$

where

$$R_1^0(\xi) = \frac{L(\xi)}{\xi}, \quad R_2^0(\xi) = \frac{L(\xi)}{\xi}Q(\sigma), \quad R_3^0(\xi) = \frac{1}{2\xi}\left(1 - 3\frac{L(\xi)}{\xi}\right)[3Q(\sigma)-1], \quad Q(\sigma) = \frac{1}{2\sigma}\left(\frac{2\exp(\sigma)}{\sqrt{\pi/\sigma}\,\mathrm{Erfi}(\sqrt{\sigma})} - 1\right),$$

$$(A_{ij}) = \begin{bmatrix} 2\tau_B s + 2 + \xi L + \dfrac{G(2+\xi L + 2\sigma Q)}{\Gamma\sigma} & -\dfrac{2G}{\Gamma} & 0 \\ \xi L Q & 2\tau_B s + 2 + \dfrac{G(\xi L + 1/Q - 1)}{\Gamma\sigma} & -\dfrac{G\xi}{\Gamma\sigma} \\ L(1-3Q)+\xi Q & -\xi & 2\tau_B s + 6 + \xi L \end{bmatrix}. \quad (44)$$

Here, Erfi is the imaginary error function. Stepanov [39] recently derived an expression coming from the extension of the study of Raikher and Shliomis in the range $\sigma < \xi/2$:

$$\mu_{\mathrm{mv}} = \frac{3}{2}\mu\varphi \frac{35L_2^2(\xi)F_2^2(\sigma)}{14+5L_2(\xi)F_2(\sigma)+16L_4(\xi)F_4(\sigma)}, \quad (45)$$

where

$$L_0 = 1, \quad L_1 = L(\xi), \quad L_{n+1} = L_{n-1}(\xi) - \frac{(2n+1)L_n(\xi)}{\xi}. \quad (46)$$

Morozov *et al.* [40] later derived a phenomenological expression proceeding from simple physical arguments, so as to improve the applicability. The simple and compact expression is given by

$$\mu_{\mathrm{mv}} = \frac{3}{2}\mu\varphi \frac{2\xi\sigma F_2(\sigma)L^2(\xi)}{2\sigma F_2(\sigma)L(\xi)[2+\xi L(\xi)]+3\xi}. \quad (47)$$

The works of Miguel and Rubí, Stepanov, and Morozov *et al.* are special cases of this study when the fluid is Newtonian (weakly nonequilibrium). In Fig. 2, we check the results for the case $\varpi\tau \to 0$ in terms of the reduced magnetoviscosity $\mu_{\mathrm{MV}} = \mu_{\mathrm{mv}}/(3\mu\varphi/2)$ with the corresponding data obtained by them. The figure shows that the four theoretical curves do not appear alike for small and moderate values of ξ, especially at small values of the magnetic-anisotropy parameter Γ (or σ). Greater values than their solutions are obtained for the hard-dipole case $\Gamma \to \infty$, but smaller values may be obtained for finite values of Γ. This means that our magnetoviscosity expression could explain a wide-ranging distribution of experimental data.

In Fig. 3, the reduced magnetoviscosity μ_{MV}, calculated from Eq. (18), is plotted as a function of the dimensionless magnetic field strength ξ for the shear deformation $\varpi\tau \to 0$, 1, and 2 with the magnetic-anisotropy parameter $\Gamma \to \infty$, 0.1, and 0.01. It is found that μ_{MV} decreased with increase of $\varpi\tau$. According to the stress-strain relation (15), the phenomenon is found to be shear thinning. The shear-thinning non-Newtonian effect causes linear viscosity variation. Decreasing the value of Γ leads to increase in the effect first and then to a decrease. The maximum non-Newtonian effect was found at Γ of the order of 0.1.

Now, we pay attention to the shear-thinning non-Newtonian effect on the flow fields and characteristics. In Fig. 4, the solid line denotes the non-Newtonian case ($\Gamma = 0.1$), and the dash-dotted line denotes the hard-dipole, Newtonian case ($\Gamma \to \infty$, $\omega\tau \to 0$). Figure 4(a) illustrates the flow fields for $\varpi\tau \to 0$, 1, and 2 with $\Gamma = 0.1$ and $\xi = 5$. It can be found from Eqs. (28), (29), (35), and (36) that, except for the velocity U^s, the field distributions are influenced by the parameter $\varpi\tau$. From the plot, the non-Newtonian effect increases slowly with the value of $\varpi\tau$ and leads to enhancement of these flow fields. Note that, on the contrary, the non-Newtonian effect leads to a reduction of the magnetization, described by Eqs. (30), (31), (37), and (38). In addition, the results reveal that the finite-magnetic-anisotropy effect is to increase the magnitudes of Ω^s, U^p, and $|\Omega^p|$ and to reduce the magnitudes of M_y^s and $|M_y^p|$.

The shear-thinning non-Newtonian effect on the flow characteristics is plotted in Fig. 4(b). It is clear from the plot and Eqs. (33) and (34) that $\hat{T}^s$ is a function of ξ, $\varpi\tau$, and Γ, but $\dot{Q}^s$ is a constant. The magnetic-field effect is to increase the magnitude of $\hat{T}^s$, but the non-Newtonian and finite-magnetic-anisotropy effects are to reduce the magnitude of $\hat{T}^s$. These variations imply that, for shear-driven flow, a comparison between the calculated results of the flow-drag solution (34) and experimental measurements provides a simple manner to determine material constants. In opposition to shear-driven flow, the pressure-driven flow rate is a function of these parameters. The magnetic-field effect is to reduce the magnitude of $\dot{Q}^p$, but the non-Newtonian and finite-magnetic-anisotropy effects are to increase the magnitude of $\dot{Q}^p$. For pressure-driven flow, comparison between the calculated results of the flow-rate solution (39) and experimental measurements provides another simple way to determine material constants.

IV. CONCLUSIONS

A magnetoviscosity expression for dilute ferrofluids with finite magnetic anisotropy has been derived by using the effective-field method. It has further been employed to develop a mathematical model of non-Newtonian flow in a planar Couette-Poiseuille system with an applied stationary uniform magnetic field oriented in the perpendicular direction of vorticity. Comparison with available Newtonian-fluid models showed that our effective-field expression can explain a wide-ranging distribution of experimental data. The stress strain relation showed that the fluid regime is shear thinning and that the maximum non-Newtonian effect could be found at the relaxation time ratio (the Néel time to the Brownian time) of the order of 0.1. It was found that the non-Newtonian effect tends to increase the velocity and angular velocity but to decrease the magnetization strength; moreover, flow rate enhancement and flow drag reduction may be obtained.

This type of study could be applicable to the determination of material constants, the understanding of ferrofluid transport behavior, and the design and fabrication of ferrohydrodynamic system devices.

ACKNOWLEDGMENT

The authors would like to acknowledge financial support from the National Science Council of Taiwan under Grant No. NSC 96-2221-E-006-052.

[1] C. P. Bean and J. D. Livingston, J. Appl. Phys. **30**, S120 (1959).
[2] R. Kaiser and G. Miskolczy, J. Appl. Phys. **41**, 1064 (1970).
[3] J. L. Neuringer and R. E. Rosensweig, Phys. Fluids **7**, 1927 (1964).
[4] K. Raj and R. Moskowitz, J. Magn. Magn. Mater. **85**, 233 (1990).
[5] B. M. Berkovsky, V. F. Medvedev, and M. S. Krakov, *Magnetic Fluids: Engineering Applications* (Oxford University Press, Oxford, 1993).
[6] Q. A. Pankhurst, J. Connolly, S. K. Jones, and J. Dobson, J. Phys. D **36**, R167 (2003).
[7] R. E. Rosensweig, *Ferrohydrodynamics* (Dover, New York, 1997).
[8] G. Bisio, G. Rubatto, and P. Schiapparelli, Energy Convers. Manage. **40**, 1267 (1999).
[9] E. E. Tzirtzilakis, Physica D **237**, 66 (2008).
[10] J. P. McTague, J. Chem. Phys. **51**, 133 (1969).
[11] M. I. Shliomis, Sov. Phys. JETP **34**, 1291 (1972).
[12] M. A. Martsenyuk, Yu. L. Raikher, and M. I. Shliomis, Sov. Phys. JETP **38**, 413 (1974).
[13] A. D. Fokker, Ann. Phys. **43**, 810 (1914).
[14] M. Planck, Sitzungsber. K. Preuss. Akad. Wiss. 324 (1917).
[15] A. O. Tsebers, Magn. Gidrodin. **20**, 343 (1984).
[16] A. O. Tsebers, Magn. Gidrodin. **21**, 357 (1985).
[17] M. A. Leontovich, *Introduction to Thermodynamics, Statistical Physics* (Nauka, Moskva, 1983).
[18] M. I. Shliomis, T. P. Lyubimova, and D. V. Lyubimov, Chem. Eng. Commun. **67**, 275 (1988).
[19] B. U. Felderhof and H. J. Kroh, J. Chem. Phys. **110**, 7403 (1999).
[20] B. U. Felderhof, Phys. Rev. E **62**, 3848 (2000).
[21] M. I. Shliomis, Phys. Rev. E **64**, 063501 (2001).
[22] H. W. Müller and M. Liu, Phys. Rev. E **64**, 061405 (2001).
[23] H. C. Weng and C. K. Chen, Phys. Rev E (to be published).
[24] R. Patel, R. V. Upadhyay, and R. V. Mehta, J. Colloid Interface Sci. **263**, 661 (2003).
[25] J. P. Embs, S. May, C. Wagner, A. V. Kityk, A. Leschhorn, and M. Lücke, Phys. Rev. E **73**, 036302 (2006).
[26] A. Leschhorn and M. Lücke, Z. Phys. Chem. **220**, 219 (2006).
[27] J. B. Hubbard and P. J. Stiles, J. Chem. Phys. **84**, 6955 (1986).
[28] P. Debye, *Polar Molecules* (Chemical Catalog Company, New York, 1929).
[29] J. Frenkel, *The Kinetic Theory of Liquids* (Dover, New York, 1955).
[30] L. Néel, Acad. Sci., Paris, C. R. **228**, 664 (1949); Ann. Geophys. (C.N.R.S.) **5**, 99 (1949).
[31] W. F. Brown, Phys. Rev. **130**, 1677 (1963).
[32] P. J. Cregg, D. S. F. Crothers, and A. W. Wickstead, J. Appl. Phys. **76**, 4900 (1994).
[33] W. T. Coffey, P. J. Cregg, D. S. F. Crothers, J. T. Waldron, and A. W. Wickstead, J. Magn. Magn. Mater. **131**, L301 (1994).
[34] P. C. Fannin and S. W. Charles, J. Phys. D **22**, 187 (1989).
[35] R. E. Rosensweig, J. Magn. Magn. Mater. **252**, 370 (2002).
[36] Yu. L. Raikher and M. I. Shliomis, J. Appl. Mech. Tech. Phys. **15**, 470 (1974).
[37] M. I. Shliomis and V. I. Stepanov, J. Magn. Magn. Mater. **122**, 196 (1993).
[38] M. C. Miguel and J. M. Rubí, Phys. Rev. E **51**, 2190 (1995).
[39] V. Stepanov, J. Magn. Magn. Mater. **258-259**, 443 (2003).
[40] K. Morozov, M. I. Shliomis, and M. Zahn, Phys. Rev. E **73**, 066312 (2006).